Octet and decuplet baryon σ-terms and mass decompositions

P. M. Copeland,[1] Chueng-Ryong Ji,[2] and W. Melnitchouk[3]

[1] *Department of Physics, Duke University, Durham, North Carolina 27708, USA*
[2] *Department of Physics, North Carolina State University, Raleigh, North Carolina 27695, USA*
[3] *Jefferson Lab, Newport News, Virginia 23606, USA*

(Dated: November 25, 2021)

We present a comprehensive analysis of the SU(3) octet and decuplet baryon masses and σ-terms using high-precision lattice QCD data and chiral SU(3) effective theory with finite range regularization. The effects of various systematic uncertainties, including from the scale setting of the lattice data and the regularization prescriptions, are quantified. We find the pion-nucleon and strange nucleon σ-terms to be $\sigma_{\pi N} = 44(3)(3)$ MeV and $\sigma_{Ns} = 50(6)(1)$ MeV, respectively. The results provide constraints on the energy-momentum tensor mass decompositions of the SU(3) octet and decuplet baryons, where we find the trace anomaly and quark/gluon energies decrease for strange baryons due to their larger strange σ-terms.

Introduction.— Matrix elements that quantify the scalar quark content of baryons are important for understanding chiral symmetry breaking in quantum chromodynamics (QCD), as well as the decomposition of baryon masses from the energy-momentum tensor (EMT) [1–4]. Usually referred to as "σ-terms", they can be used to calculate the trace anomaly of the EMT, whose existence may explain the confinement of quarks in hadrons [1, 4, 5]. They also play an important role in building dark matter models, where σ-terms often appear in the couplings of spin-1/2 dark matter particles to scalar quark bilinears [6–10]. While there are numerous reasons to have precise and accurate determinations of baryon σ-terms, in practice these have been rather difficult to determine consistently from phenomenology.

The best determined σ-terms are those of the nucleon. Its light (u and d) quark contribution, commonly referred to as the pion-nucleon σ-term, $\sigma_{\pi N}$, was determined by Gasser *et al.* [11] from an analysis of πN scattering in the early 1990s. These studies, along with σ-term extractions from chiral extrapolations of baryon mass lattice QCD data, predict a "canonical" magnitude of $\sigma_{\pi N} \approx 45$ MeV. This value is also typically supported by direct lattice simulations of $\sigma_{\pi N}$ [12]. More recent calculations of $\sigma_{\pi N}$ determined directly from pionic atom scattering experiments predict a magnitude of around 60 MeV [13, 14], in tension with the smaller canonical predictions.

The strange nucleon σ-term, σ_{Ns}, is even more controversial. Values found in the literature range from small negative to $\approx$ 300 MeV, with large uncertainties, but more recent results narrow the spread to $\sigma_{Ns} \approx$ 20–60 MeV [12, 15–18]. This range is still about twice that for $\sigma_{\pi N}$, and constitutes one of the largest sources of uncertainty when applying σ-terms, as in spin-independent WIMP-nucleon scattering [6] for instance.

One of the reasons for this uncertainty lies in the limited lattice baryon mass data available at different strange quark masses since strange σ-terms are traditionally determined from chiral extrapolations. Moreover, as highlighted by Shanahan *et al.* [16, 17], the available data can depend strongly on the lattice scale setting scheme. Attempts to minimize this dependence were made by Ren *et al.* [18] by globally fitting lattice data from different collaborations over various ranges of m_s.

Further uncertainties arise from the forms used for the chiral extrapolations of the lattice data to the physical point. In particular, the convergence of the chiral expansion as a function of the meson mass can depend on the regularization scheme chosen, and it has been argued that finite range regularization (FRR) schemes, which involve an effective resummation of higher order terms in the baryon mass, parametrized by a finite range regulator parameter, can provide better convergence over a larger range of masses [15, 19, 20]. It is also crucial to capture all intermediate π, K, and η meson states from the baryon self-energies in order to accurately describe the full light and strange quark dependence of the baryons.

In this paper, we employ the latest calculations of the octet and decuplet baryon masses within a relativistic chiral SU(3) effective theory framework [21] that uses FRR to analyze high-precision lattice QCD data from the PACS-CS [22] and QCDSF-UKQCD [23] Collaborations. Using the Feynman-Hellmann theorem [15, 16], we then use the parameters determined in the global fits to extract the light-quark and strange-quark σ-terms for all SU(3) octet and decuplet baryons, and discuss the impact of the results on baryon mass decompositions from the EMT.

Baryon masses and σ-terms.— The σ-terms for a baryon $\mathcal{B}$ are defined as the forward baryon matrix elements of a quark scalar current of flavor q,

$$\sigma_{\mathcal{B}q} = m_q \langle \mathcal{B}|\overline{q}q|\mathcal{B}\rangle, \qquad f_{\mathcal{B}q} = \frac{\sigma_{\mathcal{B}q}}{M_{\mathcal{B}}}, \tag{1}$$

where m_q and $M_{\mathcal{B}}$ are the quark and baryon masses, respectively, and $f_{\mathcal{B}q}$ are the corresponding quark mass fractions. For the nucleon, the πN and strange σ-terms are defined as $\sigma_{\pi N} \equiv \sigma_{N\ell} = m_\ell \langle N|\overline{u}u + \overline{d}d|N\rangle$ and $\sigma_{Ns} = m_s \langle N|\overline{s}s|N\rangle$, respectively, where the average light quark mass is $m_\ell = (m_u + m_d)/2$. From the m_q dependence

of the baryon masses, one can compute $\sigma_{\mathcal{B}q}$ using the Feynman-Hellmann theorem,

$$\sigma_{\mathcal{B}q} = m_q \frac{\partial M_\mathcal{B}}{\partial m_q}. \tag{2}$$

In a chiral expansion of the baryon mass one can write [15, 16],

$$M_\mathcal{B} = M_\mathcal{B}^{(0)} + \delta M_\mathcal{B}^{(1)} + \delta M_\mathcal{B}^{(3/2)} + \cdots, \tag{3}$$

where $M_\mathcal{B}^{(0)}$ is the bare baryon mass in the chiral limit, $m_q \to 0$, and $\delta M_\mathcal{B}^{(1)}$ and $\delta M_\mathcal{B}^{(3/2)}$ are quark mass dependent corrections.

The first correction is linear in the quark masses,

$$\delta M_\mathcal{B}^{(1)} = -C_{\mathcal{B}\ell}^{(1)} m_\ell - C_{\mathcal{B}s}^{(1)} m_s, \tag{4}$$

with coefficients $C_{\mathcal{B}\ell}^{(1)}$ and $C_{\mathcal{B}s}^{(1)}$ determined from the chiral SU(3) effective theory [24]. These coefficients for octet ($\mathcal{B} = B$) and decuplet ($\mathcal{B} = T$) baryons are linear combinations of the shared parameters, α, β and σ for octet, and γ and $\overline{\sigma}$ for decuplet,

$$C_{Bq}^{(1)} = a_B^q\,\alpha + b_B^q\,\beta + c_B^q\,\sigma, \tag{5a}$$

$$C_{Tq}^{(1)} = a_T^q\,\gamma + b_T^q\,\bar{\sigma}, \tag{5b}$$

where the values of the constants $a_\mathcal{B}^q$, $b_\mathcal{B}^q$, and $c_\mathcal{B}^q$ for $q = \ell, s$ are given in Ref. [24].

The $\delta M_\mathcal{B}^{(3/2)}$ term arises from the meson loop self-energies of the baryons, $\Sigma_{\mathcal{B}\mathcal{B}'\phi}$, where $\mathcal{B}'$ and ϕ denote the intermediate baryon and meson in the loop. The unique feature of this correction is that it is nonanalytic in the quark mass $m_q \sim m_\phi^2$, according to the Gell-Mann–Oakes–Renner (GOR) relation [25], with a low-energy structure that is model independent. In this work we use the latest calculations for the baryon self-energies computed within a relativistic SU(3) chiral effective theory regularized with FRR [21], which introduces an additional cutoff parameter $\Lambda_\mathcal{B}$.

To avoid mixing between the $\delta M_\mathcal{B}^{(3/2)}$ term and the lower order analytic $M_\mathcal{B}^{(0)}$ and $\delta M_\mathcal{B}^{(1)}$ terms, we "renormalize" the self-energies by subtracting the values of the $\mathcal{O}(m_\phi^0)$ and $\mathcal{O}(m_\phi^2)$ terms at $m_\phi = 0$,

$$\overline{\Sigma}_{\mathcal{B}\mathcal{B}'\phi} = \Sigma_{\mathcal{B}\mathcal{B}'\phi} - \Sigma_{\mathcal{B}\mathcal{B}'\phi}(0) - m_\phi^2 \frac{\partial \Sigma_{\mathcal{B}\mathcal{B}'\phi}}{\partial m_\phi^2}(0), \tag{6}$$

where the explicit expressions for the self-energies $\Sigma_{\mathcal{B}\mathcal{B}'\phi}$ are given in Ref. [21]. This then allows $\delta M_\mathcal{B}^{(3/2)}$ to be simply written as a sum of the renormalized self-energies over all $\mathcal{B}'$ and ϕ states,

$$\delta M_\mathcal{B}^{(3/2)} = \sum_{\mathcal{B}'\phi} \overline{\Sigma}_{\mathcal{B}\mathcal{B}'\phi}. \tag{7}$$

To preserve SU(3) symmetry, we set all octet baryon masses in the self-energy equations to the average experimental octet mass, $M_B = 1142$ MeV, and all decuplet baryon masses to their experimental average, $M_T = 1455$ GeV, which gives an octet-decuplet mass difference of 313 MeV.

Baryon mass parameters from lattice data.— To compute the $\mathcal{B}q$ σ-terms requires determining the parameters $\{M_\mathcal{B}^{(0)}, \alpha, \beta, \sigma, \gamma, \overline{\sigma}, \Lambda_\mathcal{B}\}$ in the various terms of Eq. (3), which can be done by analysing lattice QCD data on octet and decuplet baryons as a function of quark mass. Such data are available from the PACS-CS [22] and QCDSF-UKQCD [23] Collaborations, with the latter dataset for $N_f = 2 + 1$ flavors particularly useful for studying variations with both m_ℓ and m_s. In our analysis we fit the lattice baryon mass data using Eq. (3) as a function of both the π and K masses, using the GOR relation [25] to relate the quark and meson masses, $m_\ell \propto m_\pi^2/2$ and $m_s \propto m_K^2 - m_\pi^2/2$ [24, 26]. For the η meson loops in $\delta M_\mathcal{B}^{(3/2)}$, the η mass can be obtained by $m_\eta^2 \propto \frac{2}{3}(m_\ell + 2m_s) \to (4m_K^2 - m_\pi^2)/3$ [24].

When converting the data from lattice units to physical units, the method used to determine the lattice spacing a at each quark mass can have a significant impact on the magnitude of the strange quark σ-terms [17]. A standard practice for setting the scale is to assume that the lattice spacing remains fixed at each quark mass simulation point, which we refer to as the mass independent lattice spacing (MILS) scheme. In this case the lattice spacing is provided by the collaborations as $a = 0.0907$ fm for the PACS-CS points [22] and $a = 0.075$ fm for the QCDSF-UKQCD data [23]. These values are also close to those determined self-consistently using chiral EFT [27].

Alternatively, the scale can be chosen by relating it to an external quantity that is invariant under changes in the quark masses, so that any variation observed in a lattice simulation must be attributed to changes in the lattice spacing. Referring to this as the mass dependent lattice spacing (MDLS) scheme, we choose the Sommer scale $r_0 = 0.4921$ fm for the PACS-CS data [22], and the SU(3) singlet quantity $X_N = (M_N + M_\Sigma + M_\Xi)/3$ for the QCDSF-UKQCD data [23].

We apply small, finite volume corrections to both sets of data using the expressions derived in Refs. [29–31]. To minimize the effects of finite lattice volume, only data from the largest $(32^3 \times 64)$ lattice volumes are selected. Data at large m_π masses, $m_\pi^2 \gtrsim 0.25$ GeV^2, which are more susceptible to the choice of scale, are excluded. With these cuts, fitting to the PACS-CS and QCDSF-UKQCD data gives agreement between the two scale setting schemes, reducing the systematic uncertainty in σ_{Bs}.

In fitting the free parameters we allow distinct bare masses $M_B^{(0)}$ and $M_T^{(0)}$ for the octet and decuplet, respectively. The parameters α, β, σ, and $M_B^{(0)}$ are shared in the global fit of the octet, and similarly γ, $\overline{\sigma}$, and $M_T^{(0)}$

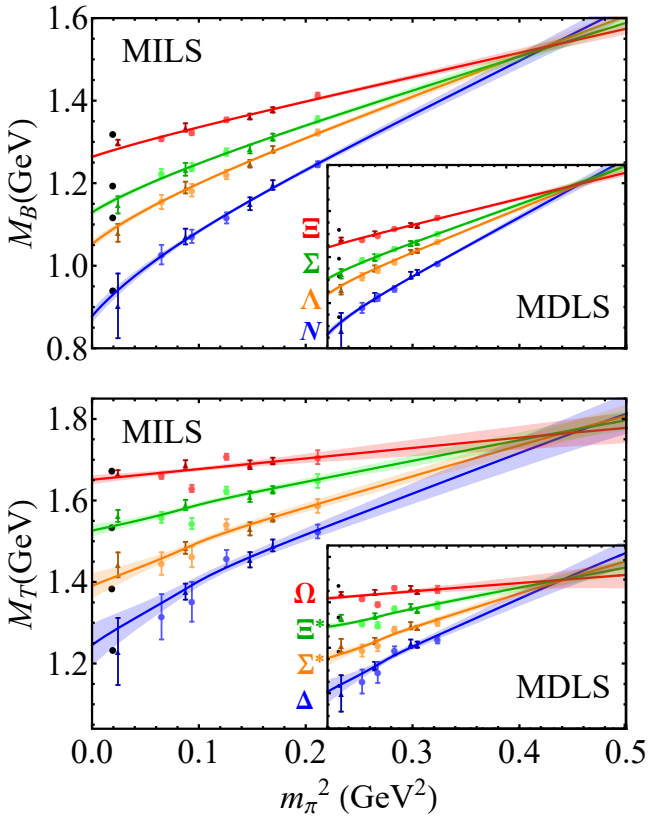

FIG. 1. Fits to the octet (top) and decuplet (bottom) baryon masses versus m_π^2 from the finite volume corrected PACS-CS [22] (lighter circles) and QCDSF-UKQCD [23] (darker triangles) data, using the MILS (main panels) and MDLS (insets) schemes. The experimental masses (black circles) are not used in the fit.

are shared in the global fit of the decuplet. In previous work [15, 16] the cutoff $\Lambda_{\mathcal{B}}$ was a shared parameter between all baryons. In the present analysis, since the cutoff does not appear in the original Lagrangian, we allow distinct $\Lambda_{\mathcal{B}}$ values to effectively parametrize the ultraviolet structure of each individual baryon $\mathcal{B}$, which is to be determined from fitting to the lattice data.

For the coupling constants, following Ref. [21] we use the values $D = 0.85$ and $F = 0.41$ the octet-octet couplings, $\mathcal{C} = \frac{6}{5} g_A$ for the octet-decuplet, and $\mathcal{H} = \frac{9}{5} g_A$ for the decuplet-decuplet coupling, with $g_A = D + F = 1.26$ the axial vector charge. For the pseudoscalar decay constant we use the convention where $f_\phi = 93$ MeV. The effects of varying the couplings within their uncertainties are relatively small [18, 28], and can be mostly compensated for by adjusting the free parameters.

The octet and decuplet baryon masses are fit to the PACS-CS [22] and QCDSF-UKQCD [23] data, and the fits presented in Fig. 1 for both the MILS and MDLS schemes. The data shown include finite volume corrections, as well as corrections for the nonphysical values of the strange quark masses used in the simulations, although the latter does not affect the fit results. Fairly good fits were obtained to the octet data, with χ^2 per degree of freedom (dof) values $\chi^2_{\rm dof} = 0.78$ and 0.89 for the MILS and MDLS schemes, respectively. The decuplet baryon data are somewhat more difficult to fit, with $\chi^2_{\rm dof} = 2.7$ and 3.3 for the MILS and MDLS cases, respectively, which mostly stems from the large spread of the lattice data and small uncertainties on the heavier baryon masses, most notably the Ω. The parameter values were found to be somewhat different for the MDLS and MILS fits (see Supplementary Material), with the latter generally giving values $\approx 100 - 200$ MeV larger than the former.

Extracted σ-terms.— From the parameters determined through the fits to the lattice QCD data, we can directly obtain predictions for the light and strange quark σ-terms. Despite differences in the parameters values for the two sets of results, the $\sigma_{\mathcal{B}q}$ values come out to be quite consistent. For the case of the nucleon, we get $\sigma_{\pi N} =$ 46(3) MeV and 41(4) MeV and $\sigma_{Ns} =$ 49(8) MeV and 50(8) MeV for the MILS and MDLS cases, respectively. This can be compared with the values $\sigma_{Ns} = 59(6)$ MeV and 21(6) MeV for the MILS and MDLS schemes obtained in Refs. [16, 17]. Note that our fits do not include experimental data points for the physical masses, which may unnaturally affect the slopes of the fitted masses due to the extremely small uncertainty on the data, explaining our somewhat larger σ_{Ns} than the $\sigma_{Ns} = 27(27)(4)$ found in Ref. [18].

The agreement between the MILS and MDLS results persists for all other baryons in the SU(3) octet and decuplet. In Table I we show the averaged values for the mass independent and mass dependent results, with differences between the two quoted as a systematic uncertainty. To explore the model dependence of the results from the renormalization prescription and the imposition of SU(3) symmetry, we in addition perform a less restricted fit in which no parameters are shared between the baryons, apart from the bare masses, $M_{\mathcal{B}}^{(0)}$, and which does not use Eq. (6) for the self-energies. This fit, which we refer to as the "generalized" scheme, gives results that are consistent with the more constrained fits described above for both MILS and MDLS. In particular, for the nucleon the πN σ-term is $\sigma_{\pi N} = 47(4)$ MeV and 45(5) MeV and the strange σ-term is $\sigma_{Ns} = 59(14)$ MeV and 68(15) MeV for the MILS and MDLS scenarios, respectively, suggesting the model used for the extrapolation of the lattice data is not overreaching (see Supplementary Material).

Our results for $\sigma_{\pi N}$ and σ_{Ns} agree well with the average $N_f = 2 + 1$ lattice values in the FLAG review [12]. On the other hand, despite our comprehensive treatment of multiple data sets, scale setting schemes and fitting models, we cannot reconcile our results with those from the Roy-Steiner equations for the πN σ-term, $\sigma_{\pi N} \approx$ 60 MeV [13, 14]. A global analysis of experimental data

TABLE I. σ-terms ($\sigma_{\mathcal{B}q}$, $q = \ell, s$), baryon masses ($M_{\mathcal{B}}$), and their ratios ($f_{\mathcal{B}q}$), together with the trace anomaly ($f_{\mathcal{B}a}$) and the sum of the quark and gluon energy contributions $\langle x\rangle^{E}_{\mathcal{B}q} + \frac{3}{4}\langle x\rangle_{\mathcal{B}g}$, extracted from fits to lattice QCD data. The first uncertainty is statistical and the second is systematic from the differences between the MILS and MDLS results.

$\mathcal{B}$ (MeV)	$\sigma_{\mathcal{B}\ell}$ (MeV)	$\sigma_{\mathcal{B}s}$ (MeV)	$M_{\mathcal{B}}$ (MeV)	$f_{B\ell}$	f_{Bs}	$f_{\mathcal{B}a}$	$\langle x\rangle^{E}_{\mathcal{B}q} + \frac{3}{4}\langle x\rangle_{\mathcal{B}g}$
$N(939)$	44(3)(3)	50(6)(1)	920(10)(10)	0.047(3)(3)	0.053(6)(1)	0.900(7)(3)	0.675(7)(3)
$\Lambda(1116)$	31(1)(2)	196(5)(7)	1080(6)(10)	0.028(1)(2)	0.176(4)(6)	0.796(4)(6)	0.597(4)(7)
$\Sigma(1193)$	25(1)(1)	256(5)(7)	1145(5)(13)	0.021(1)(1)	0.215(4)(6)	0.764(4)(6)	0.573(4)(6)
$\Xi(1318)$	15(1)(1)	365(5)(12)	1269(3)(12)	0.011(1)(1)	0.277(4)(10)	0.712(4)(10)	0.534(4)(10)
$\Delta(1232)$	29(9)(3)	67(11)(3)	1263(28)(23)	0.024(9)(2)	0.054(9)(2)	0.921(13)(3)	0.692(13)(3)
$\Sigma^*(1383)$	18(6)(2)	189(11)(9)	1385(13)(22)	0.013(4)(1)	0.137(8)(7)	0.850(9)(7)	0.638(9)(7)
$\Xi^*(1533)$	10(3)(2)	307(12)(15)	1520(6)(21)	0.007(2)(1)	0.200(8)(10)	0.793(8)(10)	0.594(8)(10)
$\Omega(1672)$	5(1)(1)	418(14)(20)	1663(8)(18)	0.003(1)(1)	0.250(8)(12)	0.747(8)(12)	0.560(8)(12)

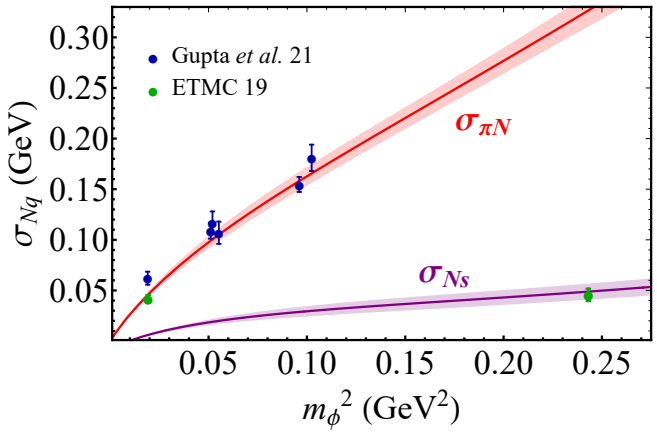

FIG. 2. Nucleon σ-terms compared with the Gupta *et al.* [32] (blue) and ETMC [33] (green) direct calculations on the lattice. The $\sigma_{\pi N}$ is plotted as a function of m_π^2 with the strange quark mass fixed, and σ_{Ns} as a function of m_K^2 with the pion mass fixed at the physical point.

and lattice simulations may be needed to obtain clarity on this difference. Recent results by Gupta *et al.* [32] have indicated that the discrepancy may be related to excited πN and $\pi\pi N$ states in direct calculations of $\sigma_{\pi N}$ on the lattice. We note, however, that SU(2) heavy baryon chiral perturbation theory is used for the computation of the scalar charge and $\sigma_{\pi N}$ in Ref. [32], while a generalization to SU(3) is required for strange quark σ-terms, $\sigma_{\mathcal{B}s}$, along with the other baryon σ-terms. Additionally, the better convergence offered by FRR could provide an improved functional form to guide the lattice calculations. In Fig. 2 we compare our MILS $\sigma_{\pi N}$ results with direct calculations from Ref. [32, 33], and the prediction for σ_{Ns} with Ref. [33], which shows good agreement all masses apart from the smallest m_π^2 results.

Baryon mass decomposition.— The quark mass fractions in Eq. (1) represent the contributions of the various quarks to the baryon mass, which is defined by the matrix elements of the EMT of QCD, $M_{\mathcal{B}} = \langle\mathcal{B}|\int d^3x\, T^{00}_{\rm QCD}|\mathcal{B}\rangle/\langle\mathcal{B}|\mathcal{B}\rangle$. This can be accordingly decomposed as [1–4],

$$M_{\mathcal{B}} = \left[\sum_q \left(\langle x\rangle^{E}_{\mathcal{B}q} + f_{\mathcal{B}q}\right) + \frac{3}{4}\langle x\rangle_{\mathcal{B}g} + \frac{1}{4}f_{\mathcal{B}a}\right] M_{\mathcal{B}}, \quad (8)$$

where $\langle x\rangle^{E}_{\mathcal{B}q} = \frac{3}{4}\left(\langle x\rangle_{\mathcal{B}q} - f_{\mathcal{B}q}\right)$ is interpreted as the quark kinetic and potential energy, and $\langle x\rangle_{\mathcal{B}q,\mathcal{B}g}$ are the quark and gluon momentum fractions of the baryons at the scale μ. The trace anomaly of the EMT, $f_{\mathcal{B}a}$, can be computed from the sum rule $f_{\mathcal{B}a} + \sum_q f_{\mathcal{B}q} = 1$ [1, 2]. Since the σ-term and trace anomaly contributions are scale independent, so is the sum, $\sum_q \langle x\rangle^{E}_{\mathcal{B}q} + \frac{3}{4}\langle x\rangle_{\mathcal{B}g} = \frac{3}{4}f_{\mathcal{B}a}$. The numerical values of the various terms in Eq. (8) are listed in Table I.

The decomposition (8) is scheme dependent and corresponds to defining the trace anomaly as the trace of the renormalized gluon component of the EMT. An alternative decomposition defines the baryons mass from only the trace of the EMT, in which case the quark and gluon energy contributions do not appear explicitly but are absorbed by the trace anomaly [4, 34]. Both of these decompostions are identical for octet and decuplet baryons, however, in a more general decomposition, such as those involving baryon gravitational form factors at zero momentum transfer, new form factors appear for the decuplet case. For the temporal component of the EMT, these terms do not contribute due to the vanishing spin polarization for the decuplet for the $\mu = 0$ component. (For spatial components, they do not vanish, and can provide information on unique anisotropic terms in the pressure/work distributions of decuplet baryons, similarly to those discussed for spin-1 hadrons [35]).

While the debate about the most appropriate mass decomposition scheme continues [4, 34, 36, 37], we note that the σ-term contribution to $M_{\mathcal{B}}$ is independent of the scheme. In Fig. 3 we use Eq. (8) to illustrate the decomposition for several representative octet and decuplet masses (nucleon, Δ, Ξ and Ω) into their trace anomaly, quark energy, and gluon momentum components.

The latter contributions decrease with increasing magnitude of the quark mass fractions for heavier baryons, so that the sum of the quark mass fractions is ≈ 3 times

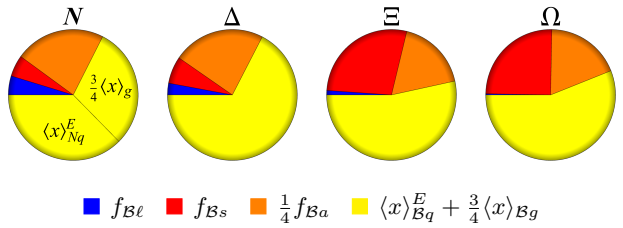

FIG. 3. Mass decomposition of the nucleon, Δ, Ξ, and Ω baryons in the rest frame, showing the fractional contributions of the light (blue) and strange (red) σ-terms, the trace anomaly (orange) and the sum of the quark and gluon energies (yellow) to the total masses of the baryons. For the nucleon, the quark and gluon contributions are shown separately, computed using PDFs from the JAM global QCD analysis [39, 40] at $\mu = 2$ GeV.

larger for the Ξ compared to the nucleon, for example. This is of particular interest as the glue energy from the trace anomaly may be associated with quark confinement in hadrons (see *e.g.*, Refs. [1, 4, 5]) by exerting a restoring pressure on the hadrons [4, 5], reminiscent of that in a bag model [1]. The decreasing magnitude of the trace anomalies for heavier baryons may indicate a proportionally smaller restoring pressure.

Outlook.— It is clear from this analysis that to better understand the internal quark and gluon compositions of baryons in QCD, the quark and gluon momentum distributions of other octet and decuplet baryons should be further studied using lattice and effective field theory techniques. Further applications of our results include constraining dark matter models, such as those involving WIMPs interacting with heavy nuclei [6, 9, 10], which require σ-terms of heavy nuclei and taking into account nuclear binding energies [7, 10]. Our results for the light and strange quark σ-terms of octet and decuplet baryons with reduced systematic uncertainty can serve as a good basis for computing the σ-terms of heavy nuclei, and in the various other applications discussed above.

Acknowledgements.— We thank A. W. Thomas, P. E. Shanahan, and R. D. Young for helpful discussions. This work was supported by the U.S. Department of Energy Contract No. DE-AC05-06OR23177, under which Jefferson Science Associates, LLC operates Jefferson Lab and DOE Contract No. DEFG02-03ER41260.

[1] X. Ji, Phys. Rev. D **52**, 271 (1995).
[2] X. Ji, Phys. Rev. Lett. **74**, 1071 (1995).
[3] Y.-B. Yang, J. Liang, Y.-J. Bi, Y. Chen, T. Draper, K.-F. Liu, and Z. Liu, Phys. Rev. Lett. **121**, 212001 (2018).
[4] K.-F. Liu, arXiv:2103.15768 [hep-ph].
[5] X. Ji, Sci. China Phys. Mech. Astron. **64**, 281012 (2021).
[6] R. J. Hill and M. P. Solon, Phys. Rev. D **91**, 043505 (2015).
[7] Z. Davoudi, W. Detmold, P. E. Shanahan, K. Orginos, A. Parreño, M. J. Savage, and M. Wagman, Phys. Rep. **900**, 0370 (2021).
[8] B. Batell, A. Freitas, A. Ismail, and D. McKeen, Phys. Rev. D **100**, 095020 (2019).
[9] M. Hoferichter, P. Klos, J. Menedez, and A. Schwenk, Phys. Rev. D **99**, 055031 (2019).
[10] S. R. Beane, S. D. Cohen, W. Detmold, H.-W. Lin, and M. J. Savage, Phys. Rev. D **89**, 074505 (2013).
[11] J. Gasser, H. Leutwyler, and M. E. Sanio, Phys. Lett. B **253**, 252 (1991).
[12] S. Aoki *et al.*, Eur. Phys. J. C **80**, 113 (2020).
[13] M. Hoferichter, J. Ruiz de Elvira, B. Kubis, and U.-G. Meißner, Phys. Rev. Lett. **115**, 092301 (2015).
[14] E. Friedman and A. Gal, Phys. Lett. B **792**, 340 (2019).
[15] R. D. Young and A. W. Thomas, Phys. Rev. D **81**, 014503 (2010).
[16] P. E. Shanahan, A. W. Thomas, and R. D. Young, Phys. Rev. D **87**, 074503 (2013).
[17] P. E. Shanahan, A. W. Thomas, and R. D. Young, PoS **LATTICE2012**, 165 (2012); arXiv:1301.3231 [hep-lat].
[18] X. L. Ren, L. S. Geng, and J. Meng, Phys. Rev. D **91**, 051502(R) (2015).
[19] J. F. Donoghue, B. R. Holstein and B. Borasoy, Phys. Rev. D **59**, 036002 (1999).
[20] R. D. Young, D. B. Leinweber, and A. W. Thomas, Prog. Part. Nucl. Phys. **50**, 399 (2003).
[21] P. M. Copeland, C.-R. Ji, and W. Melnitchouk, Phys. Rev. D **103**, 094019 (2021).
[22] S. Aoki *et al.*, Phys. Rev. D **79**, 034503 (2009).
[23] W. Bietenholz *et al.*, Phys. Rev. D **84**, 054509 (2011).
[24] A. Walker-Loud, Nucl. Phys. **A747**, 476 (2005).
[25] M. Gell-Mann, R. J. Oakes and B. Renner, Phys. Rev. **175**, 2195 (1968).
[26] P. E. Shanahan, A. W. Thomas, and R. D. Young, Phys. Rev. Lett **107**, 092004 (2011).
[27] M. F. M. Lutz, R. Bavontaweepanya, C. Kobdaj, and K. Schwarz, Phys. Rev. D **90**, 054505 (2014).
[28] A. W. Thomas, P. E. Shanahan, and R. D. Young, Few-Body Syst. **54**, 123 (2013).
[29] L. S. Geng, X.-L. Ren, J. M. Camalich, and W. Weise, Phys. Rev. D **84**, 074024 (2011).
[30] S. R. Beane *et al.*, Phys. Rev. D **84**, 014507 (2011).
[31] K.-I. Ishikawa *et al.*, Phys. Rev. D **80**, 054502 (2009).
[32] R. Gupta *et al.*, arXiv:2105.12095[hep-lat] .
[33] C. Alexandrou *et al.*, Phys. Rev. D **102**, 054517.
[34] A. Metz, B. Pasquini, and S. Rodini, Phys. Rev. D **102**, 114042 (2020).
[35] W. Cosyn *et al.*, Eur. Phys. J. C **79**, 476 (2019).
[36] C. Lorcé, Eur. Phys. J. C **78**, 120 (2018).
[37] X. Ji, Front. Phys. **16**, 64601 (2021).
[38] A. Kryjevski, Phys. Rev. D **70**, 094028 (2004).
[39] C. Cocuzza, W. Melnitchouk, A. Metz and N. Sato, Phys. Rev. D **104**, 074031 (2021).
[40] C. Cocuzza, C. E. Keppel, H. Liu, W. Melnitchouk, A. Metz, N. Sato and A. W. Thomas, arXiv:2104.06946 [hep-ph].

SUPPLEMENTARY MATERIAL

In this section we provide additional details about the fits to the lattice QCD data on baryon masses, using different lattice scale setting schemes and a generalized parametrization of the baryon masses compared to that used in Eq. (4) with chiral SU(3) constraints for $\delta M_{\mathcal{B}}^{(1)}$.

Generalized mass expansion scheme

To explore the model dependence of our analysis of the baryon masses, we consider a generalized parametrization for $M_{\mathcal{B}}$, which does not impose the constraints from SU(3) symmetry and renormalization that were used in Eqs. (4)–(7). In this alternative scenario the coefficients $C_{\mathcal{B}\ell}^{(1)}$ and $C_{\mathcal{B}s}^{(1)}$ in Eq. (4) and $\Lambda_{\mathcal{B}}$ in $\delta M_{\mathcal{B}}^{(3/2)}$ are treated as free parameters to be determined for each baryon $\mathcal{B}$ from the data. The only constraint imposed is that the bare baryon mass is the same for all baryons. Additionally, in contrast to Eq. (7), the $\delta M_{\mathcal{B}}^{(3/2)}$ term is not renormalized and is given by the direct sum over all possible intermediate states for the self-energies,

$$\delta M_{\mathcal{B}}^{(3/2)} = \sum_{\mathcal{B}'\phi} \Sigma_{\mathcal{B}\mathcal{B}'\phi}. \tag{9}$$

Since the parameters in this scheme are uncorrelated, in each self-energy term $\Sigma_{\mathcal{B}\mathcal{B}'\phi}$ we use the appropriate physical baryon mass instead of the mass averaged over the multiplet.

Fits to data

The results for the octet and decuplet baryon masses are given in Figs. 4 and 5, respectively, for the MDLS and MILS schemes, using the SU(3) constrained and generalized mass expansion schemes. Note that the SU(3) constrained results are identical to those shown in Fig. 1, which we include here for more direct comparison with the generalized results at small m_π^2 values.

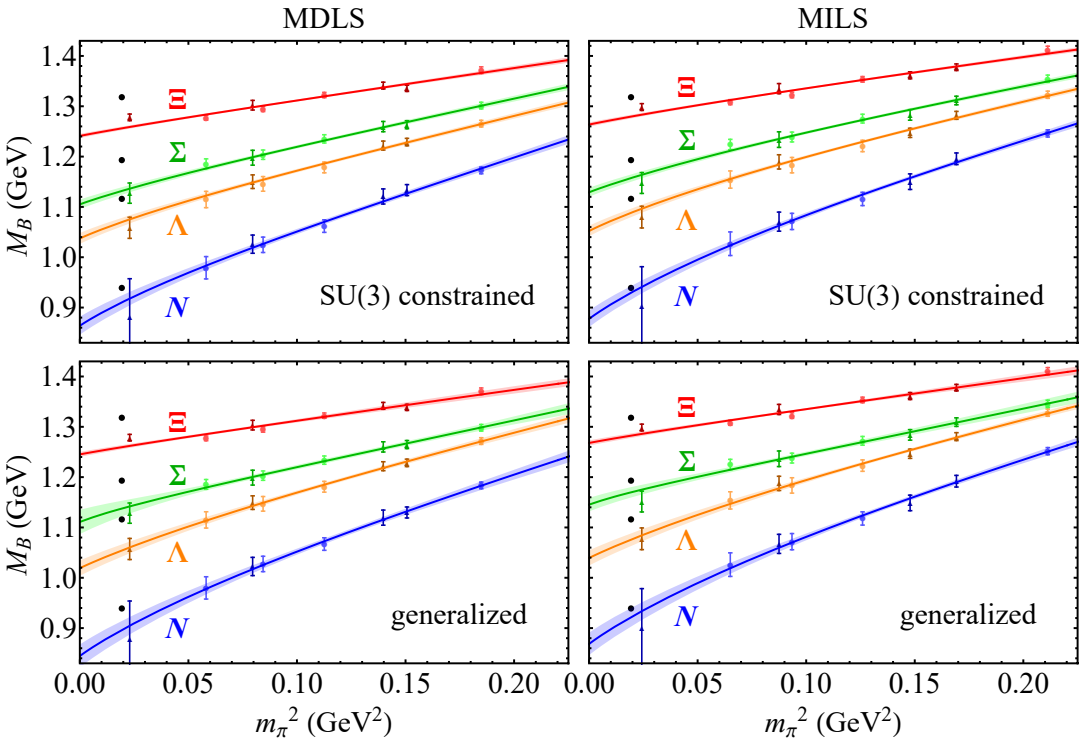

FIG. 4. Octet baryon masses versus m_π^2 for the N (blue), Λ (orange), Σ (green) and Ξ (red) baryons, for the MDLS (left) and MILS (right) schemes, with the standard SU(3) constrained (top) and generalized (bottom) mass expansion schemes. The fits are compared with PACS-CS (darker) [22] and QCDSF-UKQCD (lighter) [23] data, with the empirical values indicated by the black circles at the physical point.

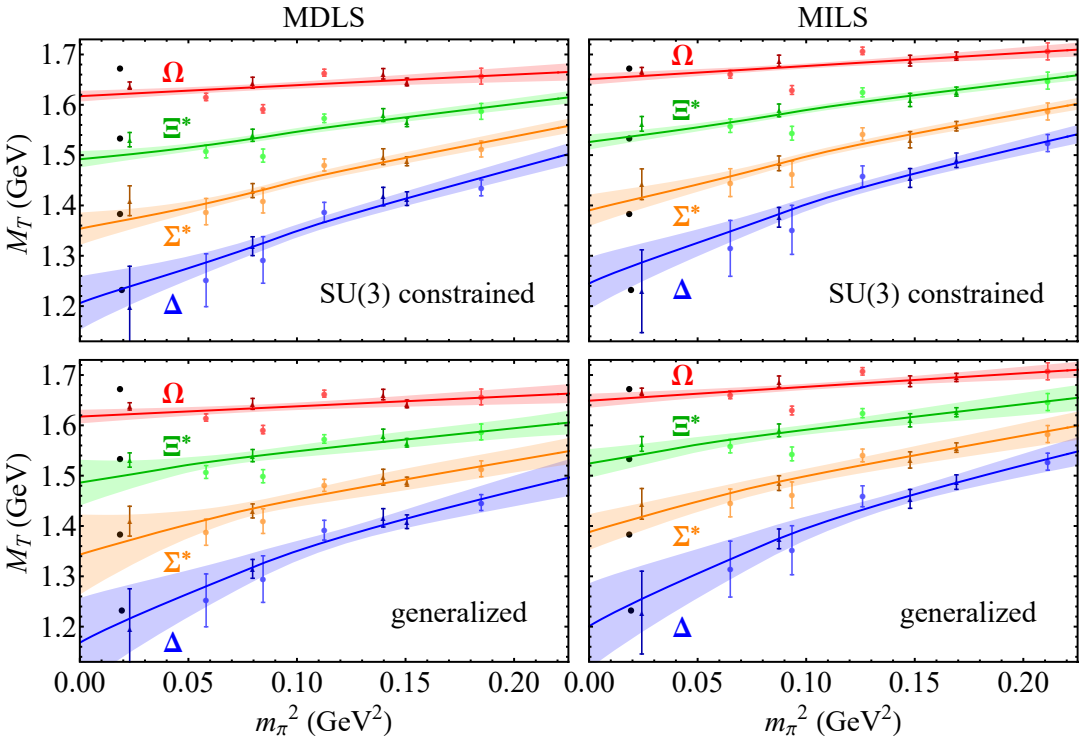

FIG. 5. As in Fig. 4, but for the decuplet baryons Δ (blue), Σ^* (orange), Ξ^* (green) and Ω (red).

Fit Parameters

The relations for the $C^{(1)}_{\mathcal{B}\ell}$ and $C^{(1)}_{\mathcal{B}s}$ coefficients in the linear quark mass term, $\delta M^{(1)}_{\mathcal{B}}$, in terms of the fit parameters α, β and σ for the octet, and γ and $\overline{\sigma}$ for the decuplet, in the SU(3) constrained scenario are given in Table II [24]. The values of the octet parameters $\{M^{(0)}_B, \alpha, \beta, \sigma, \Lambda_B\}$ and decuplet parameters $\{M^{(0)}_T, \gamma, \overline{\sigma}, \Lambda_T\}$ determined from the fits of the SU(3) constrained scheme are given in Tables III and IV, respectively. Similarly, the octet baryon parameters $\{M^{(0)}_B, C^{(1)}_{B\ell}, C^{(1)}_{Bs}, \Lambda_B\}$ and decuplet baryon parameters $\{M^{(0)}_T, C^{(1)}_{T\ell}, C^{(1)}_{Ts}, \Lambda_T\}$ determined from the fits to the lattice data using the generalized scheme are given in Tables V and VI, respectively.

TABLE II. Relations for the coefficients of the linear light quark, $C^{(1)}_{\mathcal{B}\ell}$, and strange quark, $C^{(1)}_{\mathcal{B}s}$, mass terms in terms of the fit parameters α, β, σ for the octet baryons and γ and $\overline{\sigma}$ for the decuplet baryons [24].

$\mathcal{B}$	$C^{(1)}_{\mathcal{B}\ell}$	$C^{(1)}_{\mathcal{B}s}$
N	$2\alpha + 2\beta + 4\sigma$	2σ
Λ	$\alpha + 2\beta + 4\sigma$	$\alpha + 2\sigma$
Σ	$\frac{5}{3}\alpha + \frac{2}{3}\beta + 4\sigma$	$\frac{1}{3}\alpha + \frac{4}{3}\beta + 2\sigma$
Ξ	$\frac{1}{3}\alpha + \frac{4}{3}\beta + 4\sigma$	$\frac{5}{3}\alpha + \frac{2}{3}\beta + 2\sigma$
Δ	$2\gamma - 4\overline{\sigma}$	$2\overline{\sigma}$
Σ^*	$\frac{4}{3}(\gamma - 3\overline{\sigma})$	$\frac{2}{3}(\gamma - 3\overline{\sigma})$
Ξ^*	$\frac{2}{3}(\gamma - 6\overline{\sigma})$	$\frac{2}{3}(2\gamma - 3\overline{\sigma})$
Ω	$2\gamma - 2\overline{\sigma}$	$4\overline{\sigma}$

TABLE III. Octet baryon fit parameters $M_B^{(0)}$, α, β, σ, and the regulators Λ_N, Λ_Λ, Λ_Σ, and Λ_Ξ, for the SU(3) constrained mass expansion scheme and for the MDLS and MILS scenarios. Statistical uncertainties are given in parentheses.

	$M_B^{(0)}$ (MeV)	α (MeV^{-1})	β (MeV^{-1})	σ (MeV^{-1})	Λ_N (MeV)	Λ_Λ (MeV)	Λ_Σ (MeV)	Λ_Ξ (MeV)
MDLS	799(27)	−1 362(100)	−1 097(85)	−433(53)	535(81)	545(83)	544(78)	555(83)
MILS	794(26)	−1 471(71)	−1 241(63)	−513(43)	687(70)	695(70)	703(66)	708(70)

TABLE IV. Decuplet baryon fit parameters $M_T^{(0)}$, γ, $\overline{\sigma}$, and the regulators Λ_Δ, Λ_{Σ^*}, Λ_{Ξ^*}, and Λ_Ω, for the SU(3) constrained mass expansion scheme and for the MDLS and MILS scenarios. Statistical errors are given in parentheses.

	$M_T^{(0)}$ (MeV)	$\overline{\sigma}$ (MeV^{-1})	γ (MeV^{-1})	Λ_Δ (MeV)	Λ_{Σ^*} (MeV)	Λ_{Ξ^*} (MeV)	Λ_Ω (MeV)
MDLS	1 122(93)	252(366)	−1 377(467)	483(89)	487(91)	490(94)	492(100)
MILS	1 136(91)	462(267)	−1 500(364)	549(101)	548(100)	549(103)	552(107)

TABLE V. Octet baryon fit parameters $M_B^{(0)}$, $C_{B\ell}^{(1)}$, $C_{Bs}^{(1)}$, and Λ_B ($B = N$, Λ, Σ, Ξ) for the generalized baryon mass expansion scheme.

	B	$M_B^{(0)}$ (MeV)	$C_{B\ell}^{(1)}$ (MeV^{-1})	$C_{Bs}^{(1)}$ (MeV^{-1})	Λ_B (MeV)
MDLS	N	870(32)	−2 738(256)	−281(58)	678(118)
	Λ		−2 186(199)	−869(55)	680(110)
	Σ		−1 858(302)	−1 108(66)	442(417)
	Ξ		−1 226(229)	−1 631(114)	448(136)
MILS	N	927(26)	−2 620(192)	−233(52)	730(92)
	Λ		−2 108(153)	−782(44)	734(238)
	Σ		−1 801(178)	−992(80)	387(69)
	Ξ		−1 234(179)	−1 491(80)	494(158)

TABLE VI. Decuplet baryon fit parameters $M_T^{(0)}$, $C_{T\ell}^{(1)}$, $C_{Ts}^{(1)}$, and Λ_T ($T = \Delta$, Σ^*, Ξ^*, Ω) for the generalized baryon mass expansion scheme.

	T	$M_T^{(0)}$ (MeV)	$C_{T\ell}^{(1)}$ (MeV^{-1})	$C_{Ts}^{(1)}$ (MeV^{-1})	Λ_T (MeV)
MDLS	Δ	1 184(39)	−2 014(544)	−370(191)	601(224)
	Σ^*		−1 478(547)	−851(202)	508(459)
	Ξ^*		−898(455)	−1 377(145)	499(652)
	Ω		−407(272)	−1 861(160)	540(423)
MILS	Δ	1 254(54)	−2 027(545)	−294(171)	636(214)
	Σ^*		−1 545(456)	−733(199)	500(82)
	Ξ^*		−1 002(400)	−1 238(185)	494(124)
	Ω		−541(251)	−1 698(191)	582(511)

σ-term results

The octet baryon σ-terms and masses obtained from the fitted parameters in Tables III–VI for the SU(3) contrained and generalized mass expansion schemes, and for the MDLS and MILS scenarios, are listed in Table VII, along with the χ^2 per degree of freedom ($\chi^2_{\rm dof}$) values. The corresponding decuplet baryon results are given in Table VIII.

TABLE VII. Octet baryon σ-terms and masses from the SU(3) contrained and generalized schemes, for the MDLS and MILS scenarios, along with the corresponding $\chi^2_{\rm dof}$ values.

		MDLS				**MILS**			
	B	$\sigma_{B\ell}$ (MeV)	σ_{Bs} (MeV)	M_B (MeV)	$\chi^2_{\rm dof}$	$\sigma_{B\ell}$ (MeV)	σ_{Bs} (MeV)	M_B (MeV)	$\chi^2_{\rm dof}$
SU(3) constrained									
	N	41(4)	50(8)	910(14)		46(3)	49(8)	930(14)	
	Λ	29(2)	203(7)	1 070(8)	0.89	32(2)	189(7)	1 089(8)	0.78
	Σ	24(2)	263(7)	1 132(7)		26(2)	248(7)	1 158(7)	
	Ξ	14(1)	376(7)	1 257(3)		15(1)	353(6)	1 280(4)	
generalized									
	N	46(5)	68(15)	896(18)		47(4)	59(14)	921(18)	
	Λ	32(7)	212(12)	1 055(12)	0.82	34(3)	200(13)	1 076(12)	0.75
	Σ	23(8)	257(11)	1 138(15)		21(3)	228(22)	1 170(10)	
	Ξ	14(1)	379(16)	1 260(4)		14(1)	348(17)	1 283(4)	

TABLE VIII. Decuplet baryon σ-terms and masses from the SU(3) contrained and generalized schemes, for the MDLS and MILS scenarios, along with the corresponding $\chi^2_{\rm dof}$ values.

		MDLS				**MILS**			
	T	$\sigma_{T\ell}$ (MeV)	σ_{Ts} (MeV)	M_T (MeV)	$\chi^2_{\rm dof}$	$\sigma_{T\ell}$ (MeV)	σ_{Ts} (MeV)	M_T (MeV)	$\chi^2_{\rm dof}$
SU(3) constrained									
	Δ	26(13)	69(17)	1 240(38)		31(11)	64(15)	1 285(40)	
	Σ^*	16(9)	198(18)	1 363(17)	3.29	19(7)	180(14)	1 407(20)	2.70
	Ξ^*	8(5)	322(19)	1 499(9)		11(4)	292(16)	1 540(9)	
	Ω	4(2)	437(19)	1 645(10)		5(2)	398(20)	1 681(12)	
generalized									
	Δ	38(17)	88(50)	1 209(71)		40(15)	71(48)	1 245(70)	
	Σ^*	23(23)	199(46)	1 368(55)	4.39	24(8)	171(46)	1 412(29)	3.61
	Ξ^*	13(14)	321(39)	1 500(31)		14(6)	288(45)	1 539(23)	
	Ω	4(3)	435(25)	1 622(11)		5(3)	400(38)	1 655(12)	